Vol. 60: 51–62, 2014
doi: 10.3354/cr01220

CLIMATE RESEARCH
Clim Res

Published online May 19

Design of an urban monitoring network based on Local Climate Zone mapping and temperature pattern modelling

E. Lelovics[1,*], J. Unger[1], T. Gál[1], C. V. Gál[2]

[1]Department of Climatology and Landscape Ecology, University of Szeged, Szeged, Hungary
[2]College of Architecture, Illinois Institute of Technology, Chicago, Illinois, USA

ABSTRACT: The recently developed Local Climate Zones (LCZ) classification system was initially not designed for mapping, but to classify temperature observation sites. Nevertheless, as a need arose to characterize areas based on their distinct thermal climate, utilizing LCZ classes for mapping was a logical step. The objectives of this study were (1) to develop GIS methods for the calculation of different surface parameters required for LCZ classification; (2) to identify and delineate the LCZ types within the study area using the calculated parameters; and (3) to select representative station sites for an urban monitoring network utilizing both the mapped LCZs and the modelled mean annual temperature surplus pattern in Szeged, Hungary. The study used remotely sensed data, maps and GIS databases of the city and its surroundings. The basic area of calculation was the lot area polygon, consisting of a building and its close vicinity. Adjoining polygons classified with identical or similar parameters were merged to obtain LCZs of appropriate size. As a result, 6 built LCZ types were distinguished in the studied urban area. The temperature pattern in the city was provided by an empirical model. The siting of stations took both the LCZ map and the modelled temperature pattern into account. The lampposts onto which the stations were to be mounted were determined by field surveys. The bias between the temperature pattern interpolated from the 24 stations and the initially estimated distribution by the model was found to be small. LCZ mapping is the first step in the development of urban climate maps (UCMs) that carry information on the spatial distribution and magnitude of the heat stress (thermal loads) and on the ventilation ability (dynamical potential) of different urban areas.

KEY WORDS: Urban climate · Monitoring network · Local Climate Zones · LCZs · Geographic information systems · GIS methods · Modelled temperature pattern · Szeged · Hungary

1. INTRODUCTION

Urbanization and human activities affect the climate of cities. Compared to rural areas, this climate modification is most evident in near-surface air temperature (Oke 1987). An urban heat island (UHI) is traditionally defined as the temperature difference between the 'urban' city and its 'rural' surrounding (ΔT_{u-r}). However, in the heat island literature the terms 'urban' and 'rural' have no single, objective meanings. On the one hand, the simple urban/rural (u/r) distinction is not adequate because of the variety of surface properties associated to different landscapes that influence near-surface micro and local climates (Stewart 2007, 2011). As a consequence, UHI data obtained from different parts of the world are difficult to compare. On the other hand, the lack of differentiation between landscape types likewise challenges the siting and configuration of intra-urban station networks, as the complexity and variety of the urban terrain also results in climatic differences (Oke 2004).

*Corresponding author: lelovics.eniko@gmail.com

To address these questions, Stewart & Oke (2012) developed the Local Climate Zone (LCZ) classification system. The system is based on the earlier works of Auer (1978), Ellefsen (1991), Oke (2004) and Stewart & Oke (2009), as well as on a world-wide survey of heat island measurement sites and their local settings (Stewart 2011). The primary purpose of this system is to characterize local environments around weather stations in terms of the extent to which these environments influence the local thermal climates.

LCZs are defined as 'regions of uniform surface cover, structure, material, and human activity that span hundreds of meters to several kilometers in a horizontal scale. Each LCZ has a characteristic screen-height temperature regime that is most apparent over dry surfaces, on calm, clear nights, and in areas of simple relief' (Stewart & Oke 2012). Each climate zone is necessarily 'local' in spatial scale because typically a 200 to 500 m upwind fetch is required for the air at screen-height to become fully adjusted to the underlying, relatively homogeneous surface. Based on objective, measurable parameters the authors distinguished 17 climate classes: 10 'built' type classes for urban areas and 7 'land cover' type classes for landscapes that are not built on. The characteristics of the underlying landscapes associated with each climate class are reflected in class names (e.g. 'compact mid-rise' and 'low plants' denote specific 'built' and 'land cover' type classes, respectively).

The LCZ types can be distinguished on the basis of their physical properties. The parameters used in classification are listed in Table 1. Most of these parameters characterize the surface cover and geometry of a site, while others reflect the thermal, radiative and anthropogenic energy attributes of an area. Stewart & Oke (2012) defined the typical range of properties for each zone.

The introduction of the LCZ classification system refined and standardized the way UHI is measured and documented. In this new context, the intra-urban UHI intensity is no longer an arbitrary 'urban–rural' temperature difference (ΔT_{u-r}), but a difference between distinct LCZs ($\Delta T_{LCZ\ x-y}$) (Stewart et al. 2014). Depending on the combination of the 2 selected LCZ classes, this difference can yield various outcomes. The LCZ classification system provides a method to objectively compare the thermal characteristics of different areas both within (intra-urban) and between cities (inter-urban).

In connection with weather stations sites, the classification of the surrounding urban areas generally arise in 2 situations. First, in case of existing networks (e.g. Schroeder et al. 2010, Siu & Hart 2013), the requirement to characterize the wider environment of measurement sites might emerge. The question is generally whether the measured data are typical of the site's greater area. Second, in case of planned station networks (e.g. Unger et al. 2011), the most important question is whether there is a suitable site to represent the thermal characteristics of a given area.

The LCZ classification system was initially not designed for mapping; however, in the case of the design of a new urban observation network, utilizing LCZ classification in the spatial mapping of a city is justifiable. The introduced classes support the categorization of the urban terrain, the identification of relatively homogeneous areas with respect to their surface properties, and of sites that are representative of those areas. The studies in Hamburg, Germany (Bechtel & Daneke 2012), and Xuzhou, China (Gamba et al. 2012), were among the first steps in the automated LCZ classification of urban environments using applied geographic information system (GIS) and remote sensing methods.

The present study is part of the EU-founded research (URBAN-PATH; http://urban-path.hu), which supports the development of urban monitoring systems that provide online information on the spatial distribution of temperature, humidity and human thermal comfort conditions within Szeged and Novi Sad, Serbia (Lazi et al. 2006). The siting of the planned networks' temperature and relative humidity stations (24 members in Szeged and 28 in Novi Sad) will take the surface characteristics of the surrounding sites into considerations.

This paper has 3 objectives: (1) to develop GIS methods to calculate geometrical, surface cover and radiative parameters necessary for LCZ classification with the use of available and specially created databases; (2) to identify and delineate the LCZ types within

Table 1. Zone properties of the Local Climate Zone system. Source: Stewart & Oke (2012)

Type of properties	
Geometric, surface cover	Thermal, radiative, metabolic
Sky view factor	Surface admittance (J m^{-2} s$^{-1/2}$ K^{-1})
Aspect ratio	Surface albedo
Building surface fraction (%)	Anthropogenic heat output (W m^{-2})
Impervious surface fraction (%)	
Pervious surface fraction (%)	
Height of roughness elements (m)	
Terrain roughness class	

the study area on the basis of surface parameters calculated with the help of the developed GIS methods; and (3) to select representative sites for the planned urban monitoring network based on both the mapped LCZs and the modelled mean annual temperature surplus pattern.

2. METHODS

2.1. Study area and earlier temperature measurements

Szeged is located in the south-eastern part of Hungary (46°N, 20°E) at 79 m above sea level on a flat terrain. It has a population of 160 000 and an urbanized area of about 40 km^2 (Fig. 1). The area is in Köppen's climatic region Cfb (temperate warm climate with a rather uniform annual distribution of precipitation). The annual mean temperature is 10.4°C and the mean annual amount of precipitation is 497 mm (Unger et al. 2001). The 10 × 8 km (80 km^2) rectangular study area covers Szeged and part of its surroundings (Fig. 1).

Temperature data for validation were obtained from earlier studies involving mobile measurement, carried out using cars on established traversing routes (e.g. Sümeghy & Unger 2003a,b, Unger 2004). The measurements took place at a fixed time after sunset several times during a 1 yr period (April 2002 to March 2003). The recorded observations were transformed to a uniform grid laid over the study area. From the group of measurements performed on clear and calm nights that were also preceded by at least 2 d of similar conditions, we selected 4 cases for validation. This method ensured that on selected nights, weather conditions (especially temperature) favored the development of particular thermal conditions in the near-surface air layer, influenced by the underlying surfaces.

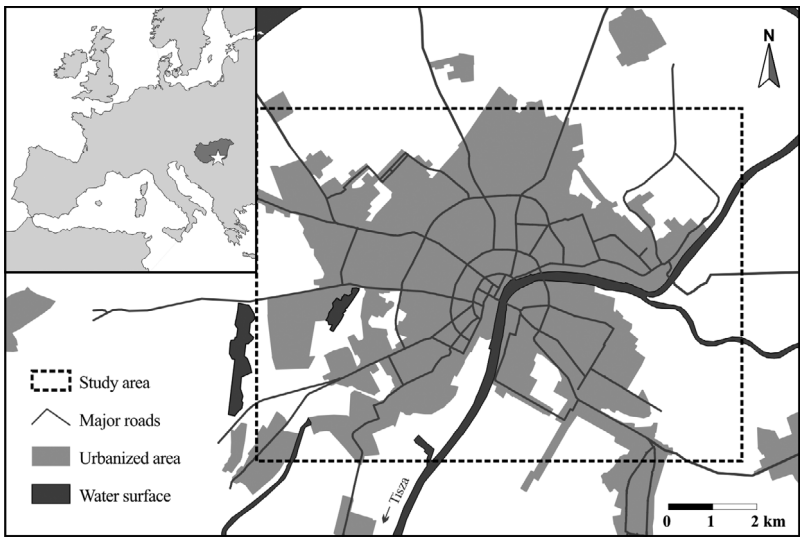

Fig. 1. Study area in and around Szeged, Hungary (bordered by dashed line), Inset: Szeged (☆) in Hungary and Europe

2.2. GIS methods for LCZ mapping

2.2.1. Parameter calculations for lot area polygons

Utilizing available databases, our GIS methods can determine 7 out of the 10 properties identified by Stewart & Oke (2012). From the initial set of parameters designated for LCZ classification, we omitted the aspect ratio (height:width, H:W), surface admittance, and the anthropogenic heat output. We ignored the aspect ratio as it tends to be too theoretical, and it can only be clearly calculated for regular street networks with straight streets, rectangular intersections and blocks of buildings filling in the available area between roads. Surface admittance and anthropogenic heat output were disregarded, as no data were available for the study area.

The basic area in the calculation of the remaining 7 parameters is the lot area polygon, which consists of a building and the area of influence around it. In determining the lot area polygons, a 3D building database of Szeged containing more than 22 000 individual buildings and building height information in ESRI shapefile format was utilized (Gál & Unger 2009). For buildings in physical contact with each other, the lot area polygon was determined for the entire group of buildings. In order to curtail the size of lot area polygons next to large open spaces without buildings (e.g. parks, fields, water), polygon areas that lay 100 m beyond the building encompassed by the polygon were cut off. We subsequently divided the study area according to the obtained polygons.

The calculation processes of the parameters and the utilized databases are presented below.

(1) Sky view factor (SVF) is the ratio of the radiation not absorbed by surrounding surface elements compared with all of the radiation emitted by a planar surface on the site. This study

utilized the Szeged SVF database used in Gál et al. (2009) and Unger (2009). With a vector based method, SVF was calculated at 5 m horizontal resolution for the city using the 3D building database of Szeged. The building database contains building footprint areas as polygon-type data and information on building heights that were derived with photogrammetric methods. The SVF calculation disregarded the effects of vegetation and pitched roofs, as buildings were assumed to be flat roofed. The SVF is calculated at the street level for the points not covered by buildings. These values are averaged for each lot area polygon.

(2) Building surface fraction (BSF) is the proportion of ground surface covered with buildings. It was calculated for each lot area polygon. The input values for the calculation, the building footprints and the lot area polygons, were also obtained from the 3D building database of Szeged.

(3) Pervious surface fraction (PSF) is the proportion of ground surface with pervious cover. The following data were used in the calculation: a RapidEye satellite imagery (RapidEye 2013), a 1:25 000 topographic map, a road database, and the CORINE Land Cover (CLC) database (Bossard et al. 2000). Normalized difference vegetation index (NDVI) was calculated from atmospherically corrected satellite images (at 5.16 m resolution) using bands 3 and 5 (Tucker 1979). Areas were considered covered if the NDVI remained below 0.3. Since agricultural land after harvest has a small NDVI, similarly to covered areas, the CLC dataset was used to separate out agricultural areas. The shapes of water bodies were digitized from the topographic map because in several cases the water had NDVI values very similar to those of some building materials. Since roads crossing agricultural areas do not appear in the CLC dataset and in urban areas they are often hidden by trees, in the final step asphalt roads were located using the road database.

(4) Impervious surface fraction (ISF) was derived from the building surface and the PSF using the following formula: ISF = 1 − (BSF + PSF).

(5) Height of roughness elements was calculated as a mean height of buildings weighted by the building footprints. The inputs for the calculation were also obtained from the 3D building database of Szeged.

(6) Terrain roughness class was determined using the Davenport roughness classification method (Davenport et al. 2000). This classification process is based on the principle that the roughness parameter (z_0) and the displacement height (z_d) of a certain area are approximately the same as that of areas with similar surface cover whose parameters have already been measured. This method distinguishes 8 roughness classes. In our study, lot area polygons were classified using visual interpretation of aerial photographs, the topographical map, and the building database.

(7) Surface albedo was calculated from the atmospherically corrected reflectance values of 5 bands (440–510, 520–590, 630–685, 690–730, and 760–850 nm). Broadband albedo was calculated as an average of reflectance values weighted with the integral of the radiation (ASTM 2012) within the spectral range of a given band (Starks et al. 1991, Tasumi et al. 2008). For the calculation, the RapidEye satellite image was used.

The flowchart of calculation processes, necessary databases and outcomes are shown in the upper and left hand parts of Fig. 2.

2.2.2. LCZ mapping: aggregation of lot area polygons

In the urban environment, the temperature measured at a height of 1.5 to 2 m is influenced by the surrounding source area of a few hundred meters radius (Oke 2004, Unger et al. 2010). Naturally, this rule-of-thumb approach depends on the spatial characteristics of the urban environment. For example, in the case of compact urban settings, the source area may only be tens of meters in radius, whereas in open urban situations, it may extend to a few hundred meters. The size of the source area also depends on weather and stability conditions (Oke 2004).

In line with this and the requirement of large homogeneous areas for establishing LCZs, lot area polygons classified into identical or similar LCZ classes were merged into zones. Thus, the requirement that prescribes stations to be located at least 250 m from the edge of the zone can be met. The relatively homogeneous surroundings of the site with a radius ≥250 m constitutes the source area of the station.

The procedure adopted to obtain LCZ areas with appropriate size is as follows: (1) The previously established lot area polygons were classified separately.

From the computed surface parameters, areal mean or percentage values were calculated for each polygon. Based on the typical parameter ranges defined by Stewart & Oke (2012) for each LCZ class, the polygons also received a score between zero and 7 indicating their fitness to a certain LCZ class (Fig. 3). When a polygon obtained high enough scores (>3.0),

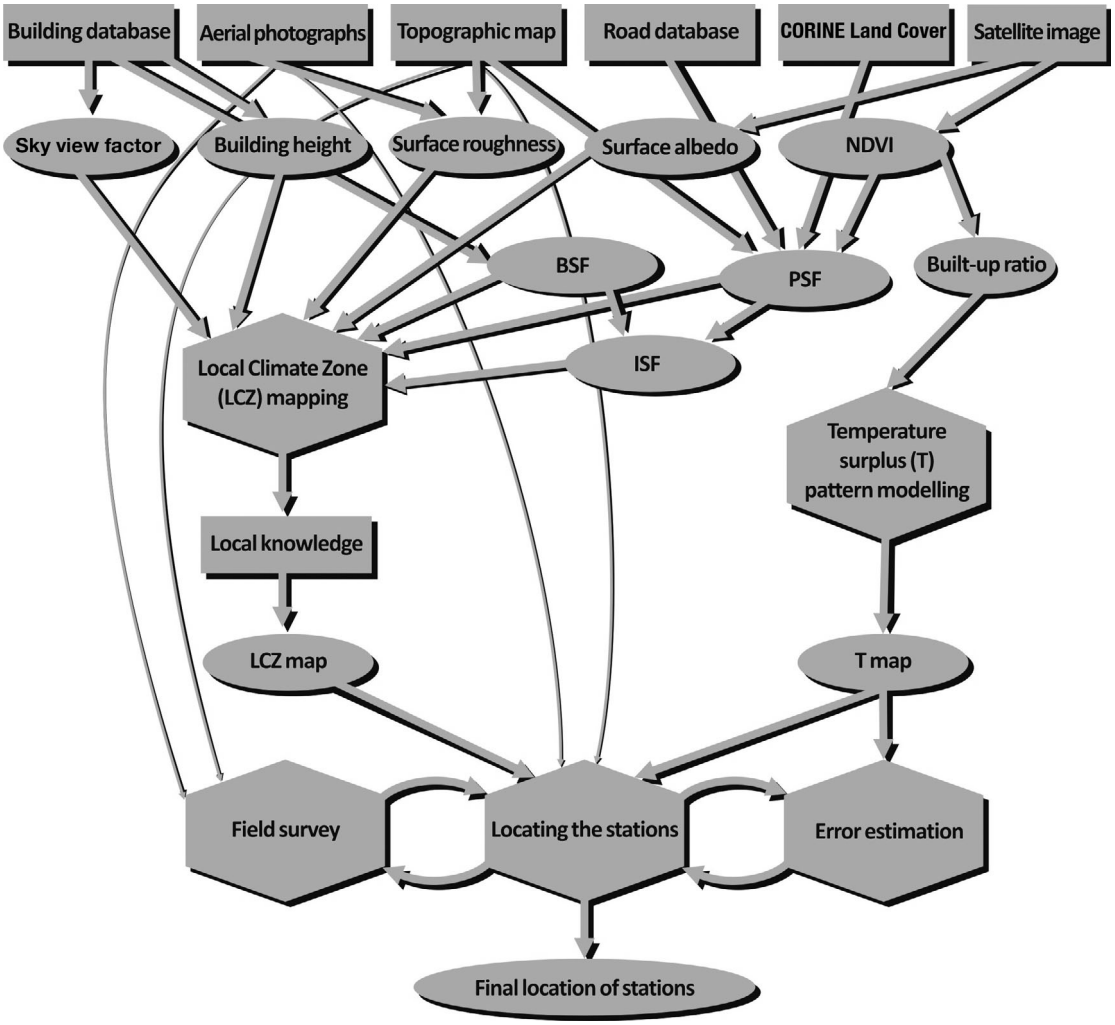

Fig. 2. Process for selecting the representative sites for the temperature monitoring network in Szeged, Hungary. NDVI: normalized difference vegetation index; BSF: building surface fraction; PSF: pervious surface fraction; ISF: impervious surface fraction

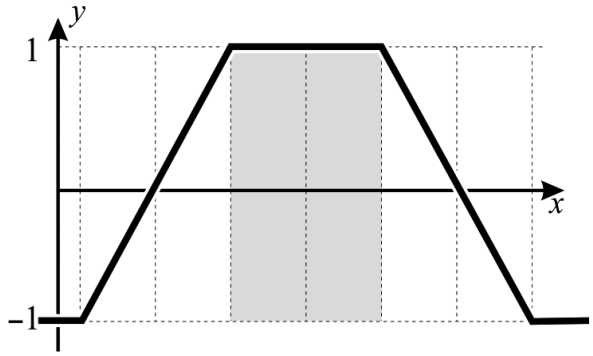

Fig. 3. Function of score assignment to a polygon according to its surface parameters. Value *x*: calculated parameter (e.g. sky view factor) of the polygon; *y*: score; solid line: score function of this polygon-parameter-LCZ combination; dark background: range of typical values for *x* in an LCZ category (from Stewart & Oke 2012)

it became associated with the 2 best fitting LCZ classes (LCZ_x indicating the best match and LCZ_y the second best). When scores were too low to meet above requirement, polygons were regarded as unclassified.

(2) Lot area polygons were merged according to their LCZ category and their location relative to each other.

(i) If a lot area polygon was located inside another polygon, then the LCZ class of the inner polygon was set the same as that of the greater polygon.

(ii) If all of the neighbors of a polygon (except perhaps one of them) belonged to the same LCZ class, then the central polygon acquired the class of its neighbors.

(iii) If a polygon did not have a neighbor of the same class, there were 2 possible outcomes: (a) When

the dissimilar poligon's LCZ_x was equivalent to one of its neighbor's LCZ_y, or *vice versa* (i.e. the polygon's LCZ_y and the neighbour's LCZ_x were equal), then the polygon acquired the same class as the neighbor. (b) If the polygon and its neighbor belonged to a similar class in terms of their assigned LCZ_x values, then the polygon was classified as the same as its neighbor. In this context, 'similarity' refers to the condition when categories share certain properties. For example, the 'compact mid-rise' or LCZ 2 class is similar to the 'compact high-rise' (LCZ 1) and 'compact low-rise' (LCZ 3) classes, as they belong to the same density category. Likewise, the 'open mid-rise' (LCZ 5) class can also be regarded similar to LCZ 2, as they share the same height category.

(iv) The remaining non-classified and non-aggregated polygons were classified as the same as the most frequently occurring class of their neighbors.

(3) The spatial extensions of the merged polygons with identical LCZ classes were examined.

(i) If the merged polygon covered an area of at least 250 m radius, then it was regarded as an independent LCZ.

(ii) Adjacent areas that did not satisfy the above size criterion were merged regardless of their properties. If the obtained group was large enough to be regarded as an independent LCZ, it acquired the class of its most frequent constituent; otherwise it was joined to the adjacent LCZ area with which it shared the greatest part of its boundary.

While the downside of this approach is that mixed sites and LCZs with small areas are not well represented, our initial aim was to produce a generalized LCZ map for the siting of an intra-urban monitoring, where these areas are of secondary importance. The obtained LCZs were stored in ESRI shapefile format, which is suitable for producing maps and for GIS database processing.

2.3. Siting of the temperature monitoring network

2.3.1. Modelling the annual mean temperature surplus pattern

In this study, the temperature surplus is defined as the temperature excess of built-up areas in comparison with non-built areas. In order to obtain its spatial distribution in Szeged, we applied the empirical model developed as part of our earlier study (for details see Balázs et al. 2009). The model estimates the annual mean temperature surplus pattern based on a few parameters only. The necessary independent variables are the site's distance from the city boundary and the built-up ratio (BR) of its neighborhood. These parameters were determined for the 320 square grid cells (side length: 0.5 km). BR, which is defined as the ratio of surfaces covered by buildings and impervious surfaces, can be calculated either as the sum of building and ISF surface fractions (see Section 2.2.1.), or by subtracting PSF from unity. Our approach, which relies on the identification of pervious surfaces, is closer to the latter, and is especially suitable for cases where detailed information about the urban area is not available. The method utilizes NDVI values calculated from RapidEye satellite images (Section 2.2.1.) to classify the study area into 3 categories: built-up area, vegetation or water surface. BR is calculated as the ratio of built-up pixels to the total number of pixels in each grid cell.

According to the empirical model, if a grid cell and the cells around it consist of pervious surfaces only (BR of 0%), then the cell is free from urban influence and has no temperature surplus. Generally, these cells are located outside of the urbanized area. The temperature excess of those cells that contain built-up surfaces (BR $\neq$ 0%) is the function of the cell's location within the urban area and of the BR of the cell and its surrounding cells. The modelled values refer to the centre of the cells (Balázs et al. 2009). The isotherms plotted from the modelled data depict the mean annual temperature surplus distribution within the study area.

2.3.2. Determining the monitoring network sites

While searching for representative station locations, 2 major criteria were considered. (1) The sites had to be surrounded by at least 250 m wide homogeneous LCZ areas, and the number of stations per each climate zone had to be roughly proportional to the areas of different LCZs. (2) The sites had to be located near areas where high and low temperature surpluses occurred, as well as near local maxima and around spatial temperature stretches, as indicated by the temperature pattern. The flowchart of the site selection process is shown in the right hand and bottom parts of Fig. 2.

There were a few other criteria considered during site selection that generally necessitated field surveys. (1) The selected site had to be typical to the LCZ where the station was located. For instance, in the 'open low-rise' zone, the station could not be located in a large surface parking area because the properties of its surface cover differed from the char-

acteristic properties of the LCZ. This results in microclimatic differences between the measurement site and its wider environment. (2) For safety reasons the sensors had to be installed at least 4 m above the ground on arms fixed to selected lampposts. Since the air in a canyon is generally well mixed (Nakamura & Oke 1988), the effect of this height on the measured values was expected to be negligible. (3) In certain cases there were no available lampposts suitable on which to mount the stations, because the street lamps hang on overhead wires. Hence, these streets were disregarded as possible locations.

2.3.3. Estimation of interpolation error in temperature surplus patterns

The spatial distribution of the measurement stations affects the calculated temperature surplus patterns. Thus, network geometry can be a source of errors (e.g. the highest temperature values could be indicated at different locations). In order to estimate the precision of the planned monitoring network in reproducing the temperature surplus pattern of the city we applied a simple test. This test used the modelled annual mean temperature surplus pattern (Section 2.3.1.) as a reference. From the modelled temperature values of the 320 grid cells, we interpolated the temperatures for the 24 planned station sites. On the basis of these interpolated values, we attempted to reproduce the initial spatial temperature distribution for the study area. Finally, we compared the 2 temperature patterns: the reference, obtained by the empirical model (Section 2.3.1.) and the one produced from the interpolated values of possible station sites. Since the latter approach generates the temperature distribution from 24 points only, the results are less detailed. Nevertheless, the approach is suitable for estimating the precision of the planned network configuration to reproduce the main characteristics of the temperature pattern in the study area. The representativeness of the network geometry can be evaluated with the estimation of the expected geometric errors in the temperature patterns. During the site selection process, several geometric configurations were tested using this method. Some sites were fixed because of special circumstances (e.g. D-1 is the existing WMO SYNOP station of the Hungarian Meteorological Service that needed to remain in place, or Site 3-1 where there were no other siting possibilities, see Fig. 8 in Section 3.2.). Other sites could move within their assigned area (on a regular grid of 50 m within polygons with an extension of several hundred meters). We regarded as the best monitoring network configuration the one where the RMSE calculated for the built-up area was minimal, and where large deviations, if any, were limited to areas beyond the city. After identifying the measurement sites, we refined the siting of instruments utilizing our local knowledge of the study area (e.g. by taking into consideration the representativeness of the microenvironment, and by finding a suitable place for the installation of the instrument).

3. RESULTS AND DISCUSSION

3.1. LCZ map and modelled temperature surplus pattern for Szeged

Since the study area consists mostly of the city's urbanized area, the primary focus of our study was the 'built' LCZ types.

Due to the character of the city, it was expected that certain 'built' LCZ classes do not occur in Szeged. These classes are the high-rise (LCZs 1 and 4), the lightweight low-rise (LCZ 7), and the heavy industrialized (LCZ 10) classes. The general LCZ map of the city was derived with the aggregation of similar areas (described in Section 2.3.2.), complemented occasionally by the authors' knowledge of the study area. The spatial disposition of the identified 6 'built' classes within the city (LCZs 2, 3, 5, 6, 8 and 9) is presented in Fig. 4. The distribution of these zones within the urban area of Szeged (46.51 km^2) is

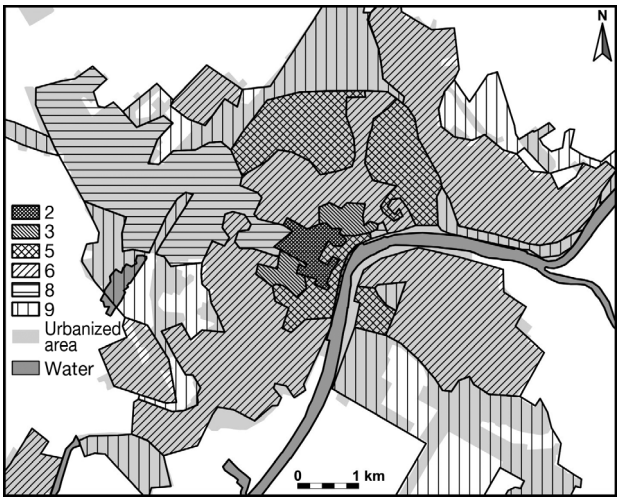

Fig. 4. Obtained Local Climate Zone (LCZ) map for Szeged, Hungary. LCZ 2: compact mid-rise, LCZ 3: compact low-rise, LCZ 5: open mid-rise, LCZ 6: open low-rise, LCZ 8: large low-rise, LCZ 9: sparsely built

as follows: 0.63, 0.67, 4.35, 19.63, 5.91, and 15.32 km^2 for LCZ 2, 3, 5, 6, 8, and 9 respectively.

In examining the relationship between the identified LCZs and the characteristic thermal conditions on those sites, we utilized the database of our earlier mobile measurement, mentioned in Section 2.2. From the available grided data points we visually selected those that, along with their surrounding area of 250 m radius, were located inside the identified LCZ zones (Fig. 5). The measured temperature values in those points served to confirm the relationship between the identified climate zones and their air temperatures. For this analysis we selected 4 nights from the available database with weather conditions that favored the development of local climates. Fig. 6 shows the average air temperature difference for the urban LCZ classes, calculated

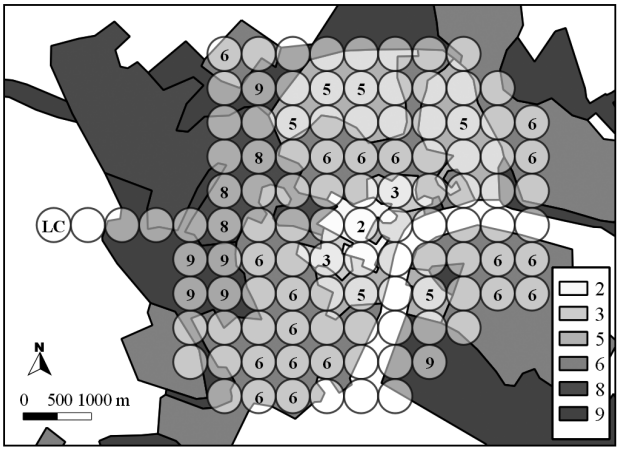

Fig. 5. Grid points of mobile measurements and their 250 m radius surroundings on the Local Climate Zone (LCZ) map of Szeged. Selected points are marked with their urban LCZ type number (see definitions in Fig. 4). LC: reference 'rural' location

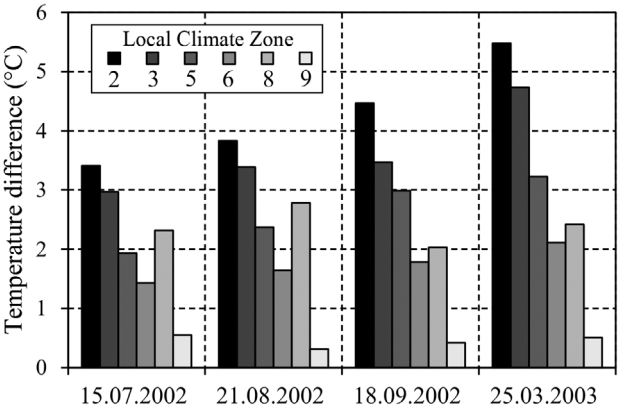

Fig. 6. Average temperature differences during 4 nights (dd.mm.yyyy) between the selected areas (circles with numbers in Fig. 5) and the remote rural location (LC) in Fig. 5. See Fig. 4 for Local Climate Zone (LCZ) definitions

between selected measurement points and the reference location (regarded as rural, and indicated by 'LC'). As expected, compact-type areas were warmer than open ones, as were mid-rise zones compared with low-rise zones. The air temperature of the sparsely built area was almost as low as the reference rural area that belongs to one of the 'land cover' type LCZ classes.

As described in Section 2.3.1., the isotherms plotted from modelled values depict the annual mean temperature surplus distribution within the study area. The thermal surplus calculated for each cell is defined in reference to grid cells of non-urban areas where the BR of the cell itself and its surroundings is 0%.

As Fig. 7 shows, the isotherms form roughly concentric curves that mirror the irregularities of the urbanized area. The highest values (>3°C) are found in the most densely built central areas.

3.2. Selection of urban monitoring network sites in Szeged

The site selection process identified 24 station sites within the study area. The distribution of stations per LCZs is as follows: 1 site in LCZs 2 and 3; 4 sites in LCZs 5 and 9; 10 sites in LCZ 6; 2 sites in LCZ 8; and 2 sites in 'land cover' type LCZ class areas, located in the western and north-eastern parts of study area (Fig. 8).

The lampposts on which to mount the stations were determined with the help of field surveys. During these surveys, we evaluated the representativeness of the lampposts' microenvironments and assessed

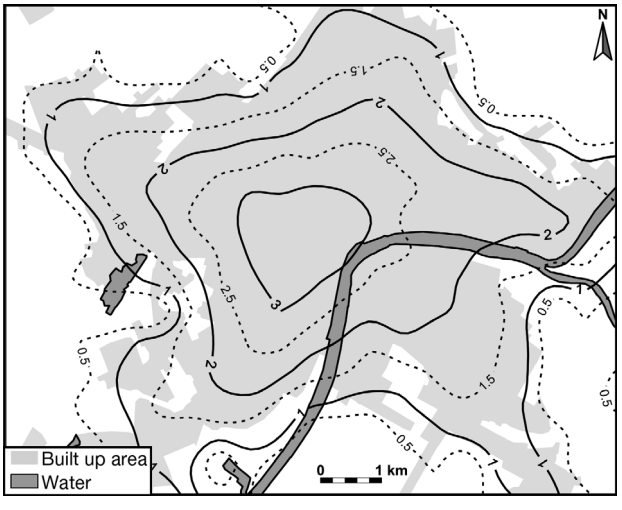

Fig. 7. Modelled temperature surplus (°C) pattern for Szeged, Hungary

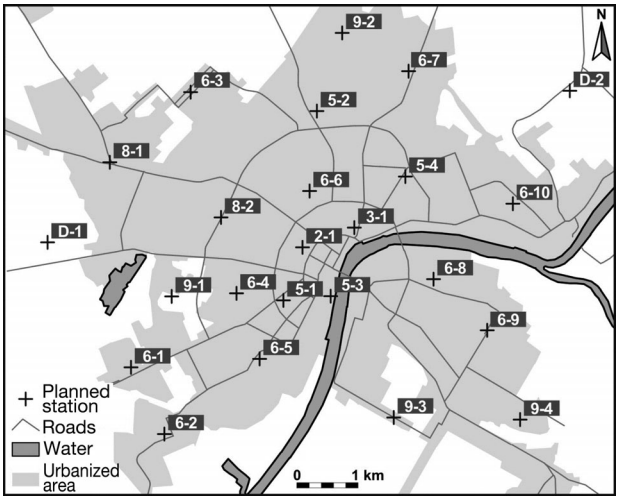

Fig. 8. Station locations of the urban monitoring network in Szeged, Hungary. Station labels: first character = LCZ type; subsequent number(s) = station no. in the given LCZ type. Stn D-1: WMO SYNOP 12982 of the Hungarian Meteorological Service

the columns' suitability for mounting the instruments (Sections 2.3.2. & 2.3.3.). The aerial photographs of 6 stations with their surroundings, representing the identified 6 'built' type LCZ classes of Szeged, are presented in Fig. 9. These pictures illustrate the spatial characteristics of these LCZs in terms of their building size and density, surface cover, etc.

3.3. Estimation of precision

The temperature surplus pattern plotted from the 24 stations' interpolated data (not shown) carries the same characteristics as the modelled reference temperature field (Fig. 7): the maximum values and their distributions are nearly identical.

The spatial distribution of the difference between the 2 temperature fields is shown in Fig. 10. According to this distribution, the monitoring network's absolute error remains below 0.5°C on 78% of the study area. Table 2 shows the frequencies of errors in detail. The area with small error corresponds to the urban part of the study area, whereas the few places of high error (≥1.5°C) occur in the rural part. The RMSE calculated for the urban area (Fig. 10) is 0.354.

The interpolation is most precise over the urban part of the city (Fig. 11). In the inner part of the study area, the error of interpolation is between −0.5 and +0.5°C. On the edge of the study area the interpolated temperature field is not as detailed as in case of the modelled distribution pattern: the isotherms are more rounded and less refined; thus, local temperature anomalies are not well represented. The reason for this difference is the sparser network density around the city's boundary, which is the outcome of the network design that primary aims at monitoring the urban area of Szeged.

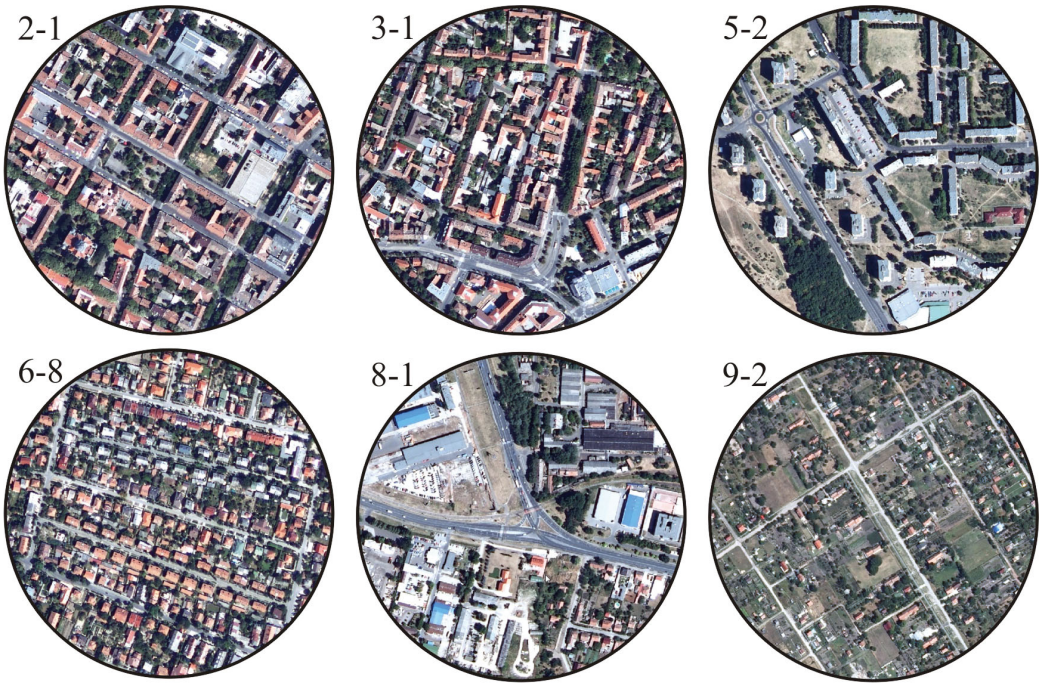

Fig. 9. Aerial photographs of the 250 m radius surroundings of 6 stations representing the 6 built LCZ types occurring in Szeged, Hungary. See Fig. 8 for station details

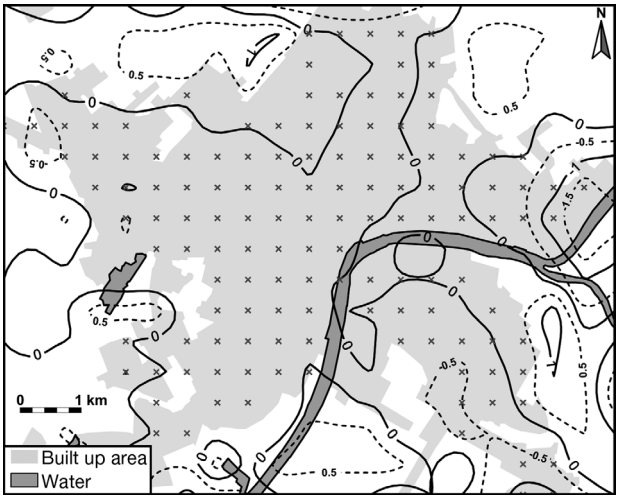

Fig. 10. Difference pattern (°C) between the modelled and interpolated temperature patterns in Szeged, Hungary. (×): grid points used in RMSE calculation (built-up area)

Table 2. Relative frequencies of the absolute error range of the monitoring network in Szeged, Hungary

Absolute error (°C)	Relative frequency (%)
0.0–0.5	78
0.5–1.0	17
1.0–1.5	4
1.5–2.0	1
>2.0	0

With linear interpolation we can determine the systematic errors of a station network caused by the network's geometry. In practice, we can reduce these kinds of errors by using the co-kriging interpolation technique (taking into consideration the surface parameters and the spatial distribution of identified LCZs) for the temperature pattern mapping in the future.

4. CONCLUSIONS

In this study we identified the representative LCZ classes of Szeged using 7 out of 10 parameters identified by Stewart & Oke (2012). The classification process relied both on developed GIS methods to calculate these values and on our knowledge of the city. As a result, 6 built LCZ types were distinguished and mapped in the studied urban area.

Within the delineated LCZ areas, 24 sites were selected as the stations of a planned urban temperature measurement network. During the selection of the sites we considered (1) the site's distance from the border of the LCZ zone within which it was located; (2) the ability of the selected network geometry to reproduce the spatial distribution of mean temperature surplus pattern estimated by an empirical model; (3) the site's representativeness of its

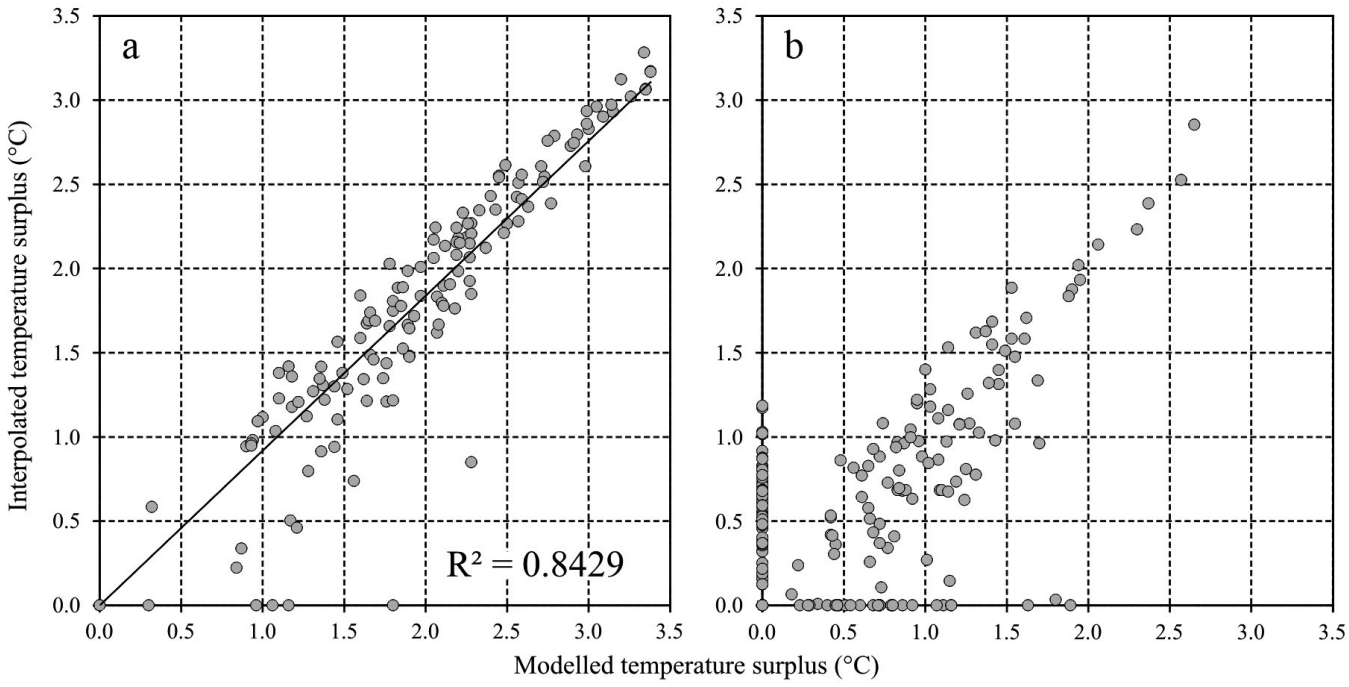

Fig. 11. Scatter-plot of the modelled and the interpolated temperature surplus of grid points on (a) built-up areas (marked '×' in Fig. 10), (b) areas that are not built-up

microenvironment; and (4) the site's suitability for instrument installation.

As a final remark, it should be mentioned that our LCZ mapping is the first step in the development of urban climate maps (see e.g. Ren et al. 2011, Acero et al. 2013). These climate maps also distinguish urban areas based on the degree of local climate modification, and carry information on the spatial distribution of heat loads and the dynamical potentials of urban areas.

Acknowledgements. The study was supported by the Hungary-Serbia IPA Cross-border Co-operation Programme (HUSRB/1203/122/166 – URBAN-PATH); E.L. was supported by the TÁMOP 4.2.4. A/2-11-1-2012-0001 'National Excellence Program – Elaborating and operating an inland student and researcher personal support system convergence program', which was subsidized by the EU and co-financed by the European Social Fund; T.G. was supported by the Hungarian Scientific Research Fund (OTKA PD-100352) and the János Bolyai Research Scholarship of the Hungarian Academy of Sciences. Special thanks are due to Dr. I. Stewart (University of Toronto) for helpful suggestions in an early stage of the manuscript.

LITERATURE CITED

Acero JA, Arrizabalaga J, Kupski S, Katzschner L (2013) Deriving an Urban Climate Map in coastal areas with complex terrain in the Basque Country (Spain). Urban Clim 4:35–60

ASTM (American Society for Testing and Materials) (2012) Reference solar spectral irradiance: air mass 1.5. http://rredc.nrel.gov/solar/spectra/am1.5 (accessed 25 Jan 2013)

Auer AH (1978) Correlation of land use and cover with meteorological anomalies. J Appl Meteorol 17:636–643

Balázs B, Unger J, Gál T, Sümeghy Z, Geiger J, Szegedi S (2009) Simulation of the mean urban heat island using 2D surface parameters: empirical modeling, verification and extension. Meteorol Appl 16:275–287

Bechtel B, Daneke C (2012) Classification of Local Climate Zones based on multiple Earth observation data. IEEE Sel Top Appl Earth Obs Remote Sens 5:1191–1202

Bossard M, Feranec J, Otahel J (2000) CORINE land cover technical guide: Addendum 2000. Tech Rep 40. European Environment Agency, Copenhagen

Davenport AG, Grimmond CSB, Oke TR, Wieringa J (2000) Estimating the roughness of cities and sheltered country. Proc 12th Conf Appl Climatol, Asheville, NC, p 96–99

Ellefsen R (1991) Mapping and measuring buildings in the canopy boundary layer in ten US cities. Energy Build 15-16:1025–1049

Gál T, Unger J (2009) Detection of ventilation paths using high-resolution roughness parameter mapping in a large urban area. Build Environ 44:198–206

Gál T, Lindberg F, Unger J (2009) Computing continuous sky view factor using 3D urban raster and vector data bases: comparison and application to urban climate. Theor Appl Climatol 95:111–123

Gamba P, Lisini G, Liu P, Du PJ, Lin H (2012) Urban climate zone detection and discrimination using object-based analysis of VHR scenes. Proc 4th GEOBIA, Rio de Janeiro, p 71–74

Lazić L, Savić S, Tomić Ž (2006) Analysis of the temperature characteristics and trends in Novi Sad area (Vojvodina, Serbia). Geogr Pannonica 10:14–21

Nakamura Y, Oke TR (1988) Wind, temperature and stability conditions in an east–west oriented urban canyon. Atmos Environ 22:2691–2700

Oke TR (1987) Boundary layer climates, 2nd edn. Routledge, London–New York, NY

Oke TR (2004) Initial guidance to obtain representative meteorological observation sites. IOM Rep 81, WMO/TD No. 1250, Geneva

RapidEye (2013) Satellite imagery product specifications, version 6.0. Blackbridge, Berlin. www.rapideye.com/upload/RE_Product_Specifications_ENG.pdf (accessed 6 May 2014)

Ren C, Ng E, Katzschner L (2011) Urban climatic map studies: a review. Int J Climatol 31:2213–2233

Schroeder AJ, Basara JB, Illston BG (2010) Challenges associated with classifying urban meteorological stations: the Oklahoma City Micronet example. Open Atmos Sci J 4: 88–100

Siu LW, Hart MA (2013) Quantifying urban heat island intensity in Hong Kong SAR, China. Environ Monit Assess 185: 4383–4398

Starks PJ, Norman JM, Blad BL, Walter-Shea EA, Walthall CL (1991) Estimation of shortwave hemispherical reflectance (albedo) from bidirectionally reflected radiance data. Remote Sens Environ 38:123–134

Stewart ID (2007) Landscape representation and urban–rural dichotomy in empirical urban heat island literature, 1950–2006. Acta Climatol Chorol Univ Szegediensis 40–41:111–121

Stewart ID (2011) A systematic review and scientific critique of methodology in modern urban heat island literature. Int J Climatol 31:200–217

Stewart ID, Oke TR (2009) A new classification system for urban climate sites. Bull Am Meteorol Soc 90:922–923

Stewart ID, Oke TR (2012) Local Climate Zones for urban temperature studies. Bull Am Meteorol Soc 93:1879–1900

Stewart ID, Oke TR, Krayenhoff ES (2014) Evaluation of the 'local climate zone' scheme using temperature observations and model simulations. Int J Climatol 34: 1062–1080

Sümeghy Z, Unger J (2003a) Seasonal case studies on the urban temperature cross-section. Acta climatologica et chorologica 36-36:01–109

Sümeghy Z, Unger J (2003b) Classification of the urban heat island patterns. Acta climatologica et chorologica 36-37: 93–100

Tasumi M, Allen RG, Trezza R (2008) At-surface reflectance and albedo from satellite for operational calculation of land surface energy balance. J Hydrol Eng 13:51–63

Tucker CJ (1979) Red and photographic infrared linear combinations for monitoring vegetation. Remote Sens Environ 8:127–150

Unger J (2004) Intra-urban relationship between surface geometry and urban heat island: review and new approach. Clim Res 27:253–264

Unger J (2009) Connection between urban heat island and sky view factor approximated by a software tool on a 3D urban database. Int J Environ Pollut 36:59–80

Unger J, Sümeghy Z, Gulyás Á, Bottyán Z, Mucsi L (2001)

Land-use and meteorological aspects of the urban heat island. Meteorol Appl 8:189–194
Unger J, Gál T, Rakonczai J, Mucsi L and others (2010) Modeling of the urban heat island pattern based on the relationship between surface and air temperatures. Idöjárás 114:287–302 (Q J Hungarian Meteorol Service)
Unger J, Savic S, Gál T (2011) Modelling of the annual mean urban heat island pattern for planning of representative urban climate station network. Adv Meteorol 2011: 398613, doi:10.1155/2011/398613

Editorial responsibility: Matthias Seaman, Oldendorf/Luhe, Germany

Submitted: September 16, 2013; Accepted: January 3, 2014
Proofs received from author(s): May 7, 2014